



ELSEVIER

Available online at www.sciencedirect.com

SCIENCE @ DIRECT®

Journal of Electrostatics 60 (2004) 97–109

Journal of
ELECTROSTATICS

www.elsevier.com/locate/elstat

A model to represent negative and positive lightning first strokes with connecting leaders

Vernon Cooray^{a,*}, Raul Montano^a, Vladimir Rakov^b

^a *Division for Electricity and Lightning Research, The Ångström Laboratory, Uppsala University, Box 539, Uppsala 751 21, Sweden*

^b *Department of Electrical and Computer Engineering, University of Florida, Gainesville, FL 32611, USA*

Abstract

A channel base current model of the current generation (CG) type is introduced to describe both negative and positive first return strokes. The key feature of the model is the association of the slow front of the channel base current waveform with the upward connecting leader. This feature is mathematically represented by a discharge propagation speed profile, which is characterized by an initial exponential increase with increasing height. It is shown that the previous models of the CG type may be incapable of reproducing adequately the observed electromagnetic fields when the channel base current contains a slow front.

© 2004 Elsevier B.V. All rights reserved.

Keywords: Lightning; Return strokes; Electromagnetic compatibility; Modelling; Electric fields; Magnetic fields

1. Introduction

Researchers use various concepts to model lightning return strokes. In one type of models, the current propagation (CP) models (also termed transmission line type models), the return stroke channel acts as a guiding structure for the current wave propagation, with the source being located at the ground [1–3]. In another type, the current generation (CG) models (also referred to as travelling current source type models), the release of the leader charge by the upward propagating return stroke front gives rise to the return stroke current [4,5,6,7,31,36]. Sometimes, most of the models in the CP and CG categories treat the channel base current as an input

*Corresponding author. Tel.: +46-18-471-58-09; fax: +46-18-471-58-10.

E-mail address: vernon.cooray@hvi.uu.se (V. Cooray).

parameter. These models are sometimes called models with specified channel base current or simply channel base current models.

In developing a mathematical model to describe first return strokes it is necessary to take into account the attachment process that involves connecting leaders. Several researchers included an upward connecting leader in their lightning models [8–11,28–30]. According to Gorin's first-stroke model [9], which belongs to the distributed circuit model category, the return stroke speed initially increases to its maximum and thereafter decreases. The initial speed increase is associated with the 'final jump' thought to be responsible for the formation of the initial rising portion of the return stroke current pulse (see also Rakov and Dulzon [3]).

In the present paper a new CG model in which the connecting leader is an integral part of the model is introduced. This model allows one to overcome some limitations of previous CG models.

2. Assumptions

- (a) The channel base (ground-level) current is known.
- (b) The charge per unit length, ρ_o , of the descending leader is independent of height (the model can readily accommodate any other charge density profile).
- (c) The slow front of the channel-base current waveform is produced by the upward connecting leader as it moves through the streamer zone of the downward extending leader. The connecting leader is launched when the streamer zone of the descending leader touches the ground. Any further extension of the descending leader channel is neglected. The connecting leader tip moves upward with an exponentially increasing speed until it makes contact with the descending leader channel.
- (d) The velocity of the return stroke above the contact point decreases exponentially with height.
- (e) The current injected into the channel at a given point on the channel, as it is passed by the upward connecting leader front (below the contact point) or by the return-stroke front (above the contact point) decays exponentially with time.
- (f) The source of current is the radial corona surrounding the descending leader core above the contact point and the streamer zone between the leader tip and the ground below the contact point.
- (g) The injected current propagates downward at the speed of light, and the current reflection coefficient at the ground is equal to zero.

3. Mathematical representation

Based on the above assumptions one can develop the necessary equations as follows. The speed of the upward connecting leader is given by

$$v_c(z) = v_o \exp(z/\lambda_c), \quad (1)$$

where v_0 is the initial speed of the connecting leader at $z = 0$ and λ_c is a constant. The final speed of the connecting leader at $z = l_c$ is

$$v_c(l_c) = v_0 \exp(l_c/\lambda_c), \tag{2}$$

where l_c is the length of the connecting leader. The return stroke starts at $z = l_c$, that is, from the contact (junction) point between the upward connecting leader and the descending leader. Thus, $v_c(l_c) = v_i$, the initial speed of the return stroke at $z = l_c$.

Since the model belongs to the CG class of models, one can show that the duration of the slow front in the channel-base current waveform, t_f , and the length of the connecting leader, l_c , are related by the equation

$$t_f = [\lambda_c(1 - \exp(-l_c/\lambda_c))/v_0] + l_c/c, \tag{3}$$

where c is the speed of light in free space. Note that Eq. (3) is based on the fact that the time t_f is equal to the time necessary for the upward connecting leader to travel the distance l_c plus the time necessary for the current to travel the distance l_c to ground. Eqs. (1)–(3) can be solved to obtain v_0 and λ_c if l_c is known. The value of l_c , the length of the connecting leader, assumed to be equal to the extension of the streamer zone of the downward-moving leader, can be calculated for any leader charge distribution by assuming that at the final jump the average potential gradient between the downward-moving leader tip and the ground is about $5\text{--}6 \times 10^5$ V/m. The average potential gradient in the gap can be calculated from the known charge distribution on the leader channel, taking into account its image in the ground. This calculation requires the radius of the leader channel. The radius of the leader channel is obtained here by assuming that the electric field at the outer boundary of the leader channel is equal to 3.0×10^6 V/m, the breakdown electric field in air at sea level. Since the velocity of the return stroke is assumed to decrease exponentially with height above $z = l_c$, one can write

$$v_r = v_i \exp(-(z - l_c)/\lambda_r), \tag{4}$$

where λ_r is the decay height constant for the return stroke speed ($z \geq l_c$).

The current per unit length injected into the channel at a given height z can be represented by [6,7]

$$I_c(z, t) = I_0(z)[e^{-t/\tau(z)}], \tag{5}$$

where $\tau(z)$ is the discharge time constant, which is a function of height, and hence the duration of the injected current. This can be expressed as

$$I_c(z, t) = \frac{\rho_0}{[\tau(z)]}[e^{-t/\tau(z)}], \tag{6}$$

where ρ_0 is the charge per unit length (assumed to be constant and the same both above and below $z = l_c$) of the descending leader. Note that in deriving Eq. (6) we have used the fact that ρ_0 is equal to the time integral (from 0 to ∞)

of the injected current. Once the velocity of the upward extending discharges (both the connecting leader and the return stroke) and the channel base current are known, the function $\tau(z)$ can be readily estimated [6]. Note that in deriving these equations it is assumed that the corona current exists from $z = 0$ and upwards whereas the hot leader tip is located at a height of l_c from ground level. The source of the corona current for z less than l_c is the charge deposited by the negative streamers in front of the hot stepped leader tip. It is also of importance to note that in the model it is assumed that the linear charge density is constant from $z = 0$ and upwards. In reality, the charge density in the streamer region may be less than that of the corona sheath. A better approximation would be to assume that the charge density increases linearly upwards reaching its maximum value at $z = l_c$ and then remains at that value along the channel. However, in the absence of information concerning the charge density in the streamer region, in the model it is assumed to be equal to that of the corona sheath.

Overall, the upward connecting leader in our model can be viewed as the initial stage of the return stroke occurring below $z = l_c$, and the propagation speed given by Eq. (1) can be interpreted as the return-stroke speed during this initial stage. Afterwards, the return-stroke speed is given by Eq. (4).

4. Input parameters: negative first strokes

On the basis of the available data on the charge distribution along the stepped leader channel, $\rho_o = 0.001$ C/m was used to represent negative first strokes [12]. The influence of this assumption on the model-predicted results is outside the scope of this paper. For the assumed charge density the estimated value of l_c is about 70 m. According to [13], the first return stroke speed averaged over channel lengths of some hundreds of meters is about 1.7×10^8 m/s with a standard deviation of 0.7×10^8 m/s. In the calculations presented in this paper it was assumed that $v_i = 2.0 \times 10^8$ m/s. This value together with the value of l_c fix v_o at 4.0×10^6 m/s, which is higher than measured speeds of upward connecting leaders of the order of 10^5 m/s [14]. However, these measured speeds are for a 200-m high object for which an upward connecting leader is expected to be initiated long before the streamer zone of the descending leader touches the object top [15]. In our model, the upward connecting leader develops entirely inside the streamer zone of the descending leader, so that the connecting leader speed may be considerably higher than for the case of upward leaders that are launched by tall objects and are developing in the virgin air. The value of λ_r was assumed to be 1500 m. The resultant average first return stroke velocity over the first kilometre of the channel is 1.4×10^8 m/s [13]. With these parameters the injected current per unit length as a function of height can be evaluated from Eq. (6). The procedure is described in [6]. The channel-base current waveform used as an input to the model is specified in Section 5 below.

5. Channel base current: negative first strokes

A waveform that can represent the channel-base current of a typical first return strokes can be described analytically using the following expression:

$$I(t) = \left\{ I_1 \frac{(t/\tau_1)^n}{1 + (t/\tau_1)^n} + I_2 [1.0 - \exp\{-t/\tau_1\}^3] \right\} \times \{a \exp(-t/\tau_2) + b \exp(-t/\tau_3)\} \quad (7)$$

with $I_1 = 7.8 \times 10^3$ A, $I_2 = 32.5 \times 10^3$ A, $n = 100$, $\tau_1 = 5.0 \times 10^{-6}$ s, $\tau_2 = 4.0 \times 10^{-6}$ s, $\tau_3 = 100.0 \times 10^{-6}$ s, $a = 0.2$ and $b = 0.8$. The current has a slow front, t_f , of about 5 μ s and a 10–90% rise time of 4.5 μ s. The charge associated with this current waveform is 3.0 C and the action integral is 4.5×10^4 A²s. These values are not much different from the corresponding median values measured for negative first return strokes [16]. The maximum derivative of the current waveform is 37 kA/ μ s, which is slightly higher than the median value, 24 kA/ μ s, for negative first strokes [16], but provides a better agreement between model-predicted and measured peak electric field derivatives at 100 km (see Section 6). If we had used a channel base current with a maximum derivative of 24 kA/ μ s [16], the peak radiation field derivative would have decreased to about 23 V/m/ μ s, somewhat smaller than the typical values obtained from measurements.

6. Model predictions: negative first strokes

Once the injected current per unit length as a function of height, the return stroke speed, and the channel base current are given, one can obtain the temporal variation of the return stroke current as a function of height along the channel [5,6]. This in turn can be used to obtain the electric and magnetic fields at any point in space. The model predicts that the peak return stroke current decreases and current rise time increases with height. This prediction is in agreement with the inferences made from optical observations. Fig. 1a shows how the peak current derivative varies with height. Note that the current derivative increases initially, reaches a peak around 70 m and decreases rapidly with further increase in height. Fig. 1b shows the time at which the peak current derivative occurs as a function of height. Note that the maximum derivative first occurs not at ground level but at the junction point between the upward connecting leader and the descending stepped leader. The current derivative reaches a peak at later times at points located below and above this junction point. This shows that establishing a contact between the upward connecting leader and the descending leader gives rise to two current waveforms, one travelling towards the cloud and the other travelling towards the ground. This is one of the important predictions of the model.

Fig. 2 shows the electric and magnetic fields at two distances from the lightning channel computed using the proposed model. These field signatures compare well with the available experimental data [17,18]. The peak derivative of the electric field

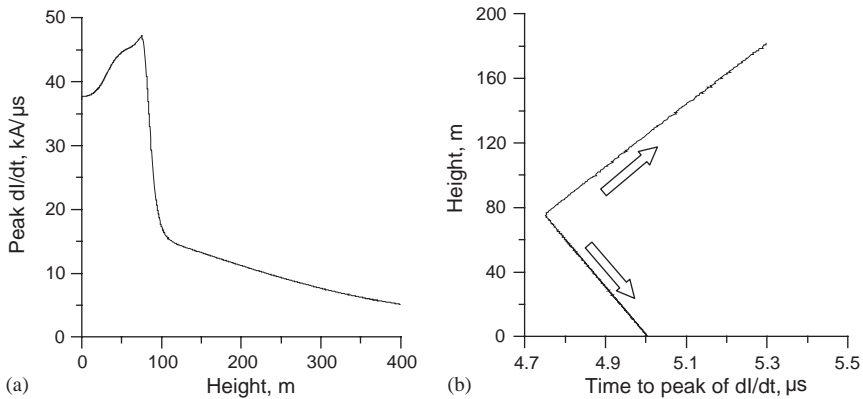


Fig. 1. (a) Variation of the peak current derivative as a function of height along the channel. (b) The time (measured from the beginning of the return stroke) at which the peak of the current derivative occurs as a function of height along the channel. Note that this represents two fast current waveforms originating at a height of 70 m (the point of contact of the connecting leader and the descending stepped leader) and travelling in opposite directions.

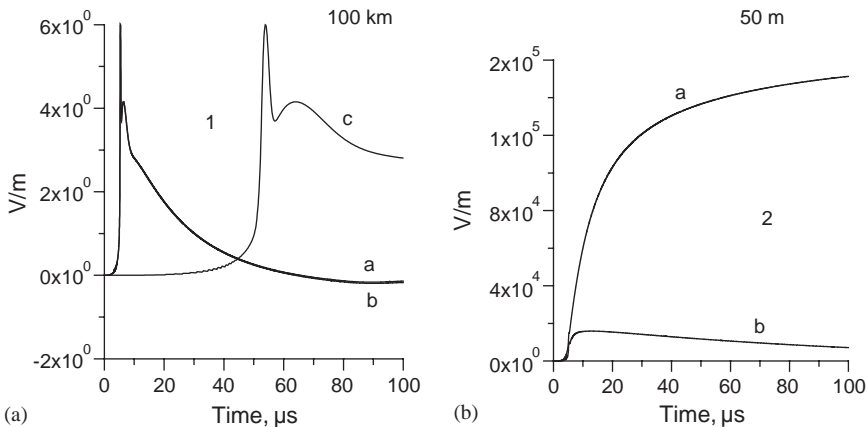


Fig. 2. (a) Vertical electric field intensity and (b) the azimuthal magnetic flux density (actually 'magnetic flux density $\times c$ ' where c is the speed of light in free space) at (1) 100 km and (2) 50 m from the negative lightning channel. Curve (c) in the left plot is an expansion of curve (a) and shows the electric field on a ten times faster time scale.

at 100 km predicted by the model is $34 \text{ V/m}/\mu s$. This agrees with the typical values obtained from measurements [19].

For comparison purposes, the electromagnetic fields predicted by the travelling current source (TCS) [4] and the Diendorfer–Uman (DU) [5] models when the same current waveform is used as an input are shown in Fig. 3. Since these latter models do not take into account the connecting leader, the velocity profile given by Eq. (4) with $l_c = 0$ was used in the calculations. In the DU model, one discharge time

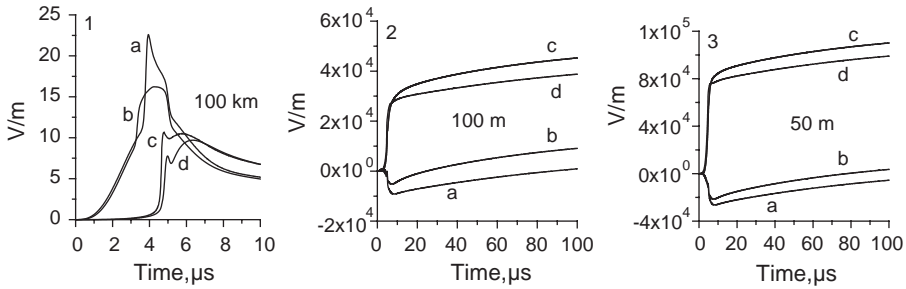


Fig. 3. Vertical electric fields at (1) 100 km, (2) 100 m and (3) 50 m as predicted by the TCS and DU models. Curves a and b show the electric fields predicted by the TCS and DU models, respectively, for the channel base current given by Eq. (7). Curves (c) and (d) show the respective field waveforms when the TCS and DU models are modified to take into account the upward connecting leader, so that the overall discharge speed profile is characterized by an exponential increase and then decrease with increasing height.

constant equal to $0.5 \mu\text{s}$ was used, but the conclusions to be drawn from the calculations are not affected by this choice. There are two significant differences between the predictions of the present model and those of the TCS and DU models. First, the electric field is positive (atmospheric electricity sign convention) at 100 km, bipolar at 100 m, and negative at 50 m for the DU model, and positive at 100 km and negative at 100 and 50 m for the TCS model. Measured electric fields within 100 m of first and subsequent return strokes, however, are positive [18,20]. Second, the electric field at 100 km exhibits an unusually large initial (radiation) peak. The radiation field peaks at 100 km are 16.5 and 23 V/m for the DU and TCS model, respectively. These values are considerably larger than measured values of 5–10 V/m. Calculations suggest that these features are caused by the presence of the slow front in the current waveform. As a result, the maximum current derivative occurs near the current peak. If the slow front is removed, the fields at 100 and 50 m become positive, and the radiation field peaks decrease to typical values.

The reason for this apparently abnormal behaviour of the TCS and DU models can be understood when one recalls that in CG models the channel base current is the sum of currents generated by elementary current sources distributed along the channel. Assume for the moment that the return stroke speed is constant. Any sudden change in the channel base current at time t is a result of a sudden change (either in amplitude or duration) at time $t - z/v$ of the injected current of channel section at height z , where $z = t/(1/v + 1/c)$. When the channel base current used as an input in the return stroke model contains a slow front of duration t_0 , which is followed by a fast transition, the model will give rise to a rapid increase in the injected current of channel segments located at height z and above, where $z = t_0/(1/v + 1/c)$. This will lead to a fast current pulse that will propagate towards the ground with the speed of light and reach the ground at $t = t_0$, causing the fast transition in the channel base current. For slow fronts having durations observed in

first return stroke current waveforms (about 5–10 μs) and for typical return stroke speeds (about 1.0×10^8 – 2.0×10^8 m/s) the origin of the injected current surge will be at heights of 400–1200 m. The downward propagation of this fast current front along many hundreds of meters of the return stroke channel will lead to the exaggeration of the distant field peaks, and the resultant excess negative charge near the bottom of the channel will lead to the change in polarity of the close fields. Interestingly, Thottappillil et al. [21] predicted that the TCS model and the DU model would generate electric fields of abnormal polarity very close to the channel due to the assumption that the current reflection coefficient at ground level is equal to zero. This latter assumption is apparently responsible for the inadequate rate of removal of charge from the bottom of the channel when the injected current surge occurs. The expected value of the current reflection coefficient at ground in a practical situation is near unity, which corresponds to nearly short-circuit conditions and assures that no excess charge can be accumulated at the bottom of the channel.

In the model presented here we associated the slow front in the channel base current waveform with the upward connecting leader. This feature is mathematically incorporated into the model as a modification of the velocity profile of the discharge. Previously, Thottappillil and Uman [22] showed that a better agreement between the initial peak of the calculated and measured radiation fields of a subsequent return stroke for the case of a current waveform containing a slow front could be obtained if the return stroke velocity was assumed to increase exponentially from a small value to the experimentally measured value. However, in contrast to the present model, they did not attempt to connect the velocity profile to the duration of the slow front of the channel base current. Note that all the channel base current models of the CG type have the velocity profile and charge distribution, or the velocity profile and the discharge time constant profile as inputs. Therefore in any model of this type, the only modification that is needed to introduce the connecting leader and hence to utilize a channel base current with a slow front, is to change the velocity profile as given in Eqs. (1)–(4) (the authors do not rule out the possibility of finding a better velocity profile for the connecting leader). The electric fields predicted by the TCS and DU models after adjusting their velocity profiles are also shown in Fig. 3 (curves c and d, respectively). Clearly, the electric fields predicted by the so modified TCS and DU models do not show the peculiar features (too large initial field peaks at far distances and the polarity reversal at close distances) that were present before this adjustment was made.

7. Positive first strokes

Both electric field and direct current measurements indicate that the main difference between the positive and negative return stroke currents is the presence of a long current tail in the former. The electric field measurements indicate that the first few tens of microseconds of the positive return stroke current is qualitatively similar to that of the negative first strokes. After this initial stage the negative current

continues to decay, whereas the positive current often starts to increase again, reaches a second peak within about 100–300 μs and decays within a few milliseconds [24]. Cooray and Lundquist [33] and Cooray [24,32] suggested that this second current enhancement is produced when the positive return stroke front encounters a large source of positive charge, probably an extensively branched and predominantly horizontal channel system in the cloud, as it extends (as a positively charged leader) beyond the origin of the flash. Rakov [25] offered a different explanation of millisecond-scale current waveforms associated with positive lightning.

A current waveform representative of positive lightning can be described analytically by the following equation:

$$I(t) = \left\{ I_1 \frac{(t/\tau_1)^n}{1 + (t/\tau_1)^n} + I_2 [1.0 - \exp\{-t/\tau_1\}^3] \right\} \\ \times \{ a \exp(-t/\tau_2) + b \exp(-t/\tau_3) \} \\ + \left\{ I_3 \frac{(t/\tau_4)^5}{1 + (t/\tau_4)^5} \exp(-t/\tau_5) \right\} \quad (8)$$

with $I_1 = 18.7 \times 10^3$ A, $I_2 = 78.0 \times 10^3$ A, $n = 100$, $\tau_1 = 15.0 \times 10^{-6}$ s, $\tau_2 = 4.0 \times 10^{-6}$ s, $\tau_3 = 100.0 \times 10^{-6}$ s, $a = 0.2$, $b = 0.8$, $I_3 = 69 \times 10^3$ A, $\tau_4 = 150 \times 10^{-6}$ s and $\tau_5 = 480 \times 10^{-6}$ s. The slow front duration, t_f , of this current waveform is 21 μs and the 10–90% rise time of this current waveform is 22 μs . This risetime is close to the typical values measured for positive return strokes [16]. The peak value of the assumed channel-base current waveform is 60 kA. This is larger than the median positive peak current of 35 kA [16]. Our choice of a relatively large peak current is based on the observation that, on average, the peak radiation fields of positive strokes are two times larger than those of negative first strokes. Since the speeds of positive return strokes do not differ significantly from those of negatives [27], a likely explanation for this observation is a factor of two higher median current for positives than for the negatives. The maximum derivative of the assumed current waveform is 30 kA/ μs . This is considerably higher than the observed median value of 2.4 kA/ μs for positives, but it will lead to model-predicted electric field derivatives similar to those measured. The associated impulse charge is 28 C which is close to the measured value for a 60 kA positive current. Note that according to Rakov [25], Berger's sample of 26 positive lightning strokes presented in [16] is a mix of two different types of lightning events. This can, at least in part, explain the apparent inconsistencies in the assumed parameters of positive strokes.

The assumed velocity profile used in calculating electromagnetic fields is similar to that used earlier for negative return strokes. Since the assumed peak current is twice that for negatives, the value of ρ_0 for positive strokes is assumed to be 0.002 C/m. This charge density results in a connecting leader length of 130 m (neglecting the polarity effect) which is larger than the upward connecting leader length obtained for negative strokes. Note that Berger observed upward connecting leaders in positive lightning up to 1–2 km in length. The electromagnetic fields predicted by the model

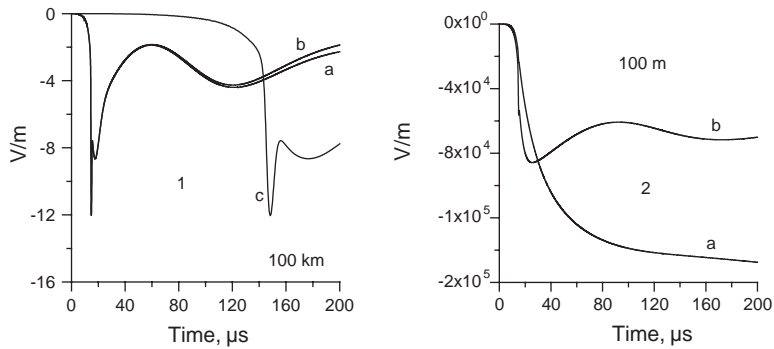


Fig. 4. (a) Vertical electric field intensity and (b) azimuthal magnetic flux density (actually 'magnetic flux density $\times 5c$ ' where c is the speed of light in free space) at (1) 100 km and (2) 100 m from the positive lightning channel. Curve (c) in the left plot is an expansion of curve (a) and shows the electric field intensity on a ten times faster time scale.

at two distances are shown in Fig. 4. The long slow front and the slow tail in the radiation field waveforms at 100 km are consistent with observations. The peak radiation field and the peak radiation field derivative at 100 km are about 12 V/m and 25 V/m/ μ s, respectively. These values agree with the typical values observed for positive strokes [26].

8. Concluding remarks

In the analysis presented here it is assumed that the upward connecting leader from the time of its inception develops entirely within the streamer zone of the descending leader. This may be true in the case of lightning strikes to flat ground, in which the streamer zone may touch the ground before the initiation of the upward connecting leader, as is the case for long sparks in rod-plane gaps. However, in the case of lightning strikes to tall towers, the connecting leader is likely to develop before the streamer zone touches the top of the tower [15].

Rakov and Uman [35] give the following description of the processes involved in the lightning attachment to a grounded object. The process by which the extending plasma channels of the upward and downward leaders make contact is called the break-through phase or final jump. This process begins when the relatively low conductivity streamer zones ahead of the two propagating leader tips meet to form a common streamer zone. The subsequent accelerated extension of the two relatively high conductivity plasma channels toward each other takes place inside the common streamer zone. The break-through phase can be viewed as a switch-closing operation that serves to launch two return-stroke waves from the point of junction between the two plasma channels. One wave moves downward, toward the ground, and the other upward, toward the cloud. The downward-moving return-stroke wave quickly reaches the ground, and the resultant upward reflected wave from ground catches up

with the upward-moving return-stroke wave from the junction point. The reflected wave from the ground propagates in the return-stroke-conditioned channel and, hence, is likely to move faster than the upward wave from the junction point that propagates along the leader-conditioned channel. When the waves bouncing between the ends of the growing return-stroke channel decay, a single upward-moving wave is formed. Thus, the lightning attachment process involves two plasma channels growing toward each other, initially in air (the upward connecting leader phase) and then inside the streamer zone (the break-through phase). It is a matter of definition whether the very short-lived bidirectional return-stroke wave should be considered a part of the attachment process or a part of the return stroke. A number of the described features of the attachment process are neglected in the model presented here. However, this model is clearly a step forward in modelling first strokes terminating on flat ground.

Weidman and Krider [23] considered the possibility that the slow front in radiation field waveforms is due to an upward connecting discharge. They estimated that such a discharge would appear to have a length in excess of 100 m and a peak current of the order of 10 kA or more. Currents in the kiloampere range associated with unconnected upward discharges from a tall object were reported by Mazur and Ruhnke [34]. On the other hand, current measurements for upward connecting leaders in flashes initiated from tall towers are typically of the order of 100 A [35]. More data are needed to resolve this apparent discrepancy.

The proposed lightning return stroke model of the CG type includes an upward connecting leader and is suitable for both negative and positive first return strokes. The new model allows one to overcome some limitations of previous CG models, such as the TCS and DU models.

References

- [1] M.A. Uman, D.K. McLain, Magnetic field of lightning return stroke, *J. Geophys. Res.* 74 (1969) 6899–6910.
- [2] C.A. Nucci, C. Mazzetti, F. Rachidi, M. Ianoz, On lightning return stroke models for LEMP calculations, 19th International Conference on Lightning Protection, Graz, Austria, 1988.
- [3] V.A. Rakov, A.A. Dulzon, A modified transmission line model for lightning return stroke field calculation, in: Proceedings of the 9th International Symposium on EMC, Zurich, Switzerland, paper 44H1, 1991, pp. 229–235.
- [4] F. Heidler, Travelling current source model for LEMP calculation, Proceedings of the 6th Symposium on EMC, Zurich, Switzerland, paper 29F2, 1965, 1985, pp. 157–162.
- [5] G. Diendorfer, M.A. Uman, An improved return stroke model with specified channel base current, *J. Geophys. Res.* 95 (1990) 13621–13664.
- [6] V. Cooray, Predicting the spatial and temporal variation of the current, the speed and electromagnetic fields of subsequent return strokes, *IEEE Trans. Electromagn. Compatibility* 40 (4) (1998) 427–435.
- [7] V. Cooray, A model for negative first return strokes in negative lightning flashes, *Phys. Scripta* 55 (1997) 119–128.
- [8] D.F. Strawe, Non-linear modeling of lightning return strokes, in: Proceedings of the Federal Aviation Administration/Florida Institute of Technology Workshop on Grounding and Lightning Technology, Melbourne, Florida, Report FAA-RD-79-6, 1979, pp. 9–15.

- [9] B.N. Gorin, Mathematical modeling of the lightning return stroke, *Elektrichestvo* 4 (1985) 10–16.
- [10] A.S. Podgorski, J.A. Landt, Three dimensional time domain modeling of lightning, *IEEE Trans. Power Delivery* 2 (1987) 931–938.
- [11] E.J. Ribeiro, G.C. Miranda, FDTD simulation of the lightning return stroke channel using a charged transmission line, in: *Proceedings of the 26th International Conference on Lightning Protection*, Cracow, Poland, 2002, pp. 56–59.
- [12] B.F.J. Schonland, The lightning discharge, in: *Handbook der Physik*, Vol. 22, Springer, Berlin, 1956, pp. 576–628.
- [13] D.M. Mach, W.D. Rust, Photoelectric return stroke velocity and peak current estimates in natural and triggered lightning, *J. Geophys. Res.* 94 (1989) 13237–13247.
- [14] S. Yokoyama, K. Miyake, T. Suzuki, S. Kanao, Winter lightning on Japan sea coast—development of measuring system on progressing feature of lightning discharge, *IEEE Trans. Power Delivery* 5 (1990) 1418–1425.
- [15] V.A. Rakov, A.O. Lutz, A new technique for estimating equivalent attractive radius for downward lightning flashes, in: *Proceedings of the 20th International Conference on Lightning Protection*, Interlaken, Switzerland, September 1990.
- [16] K. Berger, R.B. Anderson, H. Kröniger, Parameters of lightning flashes, *Electra* 40 (1975) 101–119.
- [17] Y.T. Lin, M.A. Uman, J.A. Tiller, R.D. Brantley, W.H. Beasley, E.P. Krider, C.D. Weidman, Characterization of lightning return stroke electric and magnetic fields from simultaneous two-station measurements, *J. Geophys. Res.* 84 (1979) 6307–6314.
- [18] V.A. Rakov, Lightning discharges triggered using rocket and wire techniques, *Recent Res. Dev. Geophys.* 2 (1999) 141–171.
- [19] E.P. Krider, C. Letenturier, J.C. Willett, Submicrosecond field radiated during the onset of first return strokes in cloud-to-ground lightning, *J. Geophys. Res.* 101 (D1) (1996) 1589–1597.
- [20] V.A. Rakov, M.A. Uman, D.E. Crawford, J. Schoene, J. Jerauld, K.T. Rambo, G.H. Schnetzer, B.A. DeCarlo, M. Miki, Close lightning electromagnetic environment: triggered lightning experiments, in: *Proceedings of the 15th International Zurich Symposium on EMC*, 2003, pp. 545–550.
- [21] R. Thottappillil, V.A. Rakov, M.A. Uman, Distribution of charge along the lightning channel: relation to remote electric and magnetic fields and to return stroke models, *J. Geophys. Res.* 102 (1997) 6987–7006.
- [22] R. Thottappillil, M.A. Uman, Comparison of lightning return stroke models, *J. Geophys. Res.* 98 (1993) 22903–22914.
- [23] C. Weidman, E.P. Krider, Submicrosecond risetimes in lightning return stroke fields, *J. Geophys. Res. Lett.* 7 (1980) 955–958 (Correction: *J. Geophys. Res.* 87 (1982) 7351.).
- [24] V. Cooray, Further characteristics of positive radiation fields from lightning in Sweden, *J. Geophys. Res.* 84 (1984) 11807–11815.
- [25] V.A. Rakov, A review of positive and bipolar lightning discharges, *Bull. Amer. Meteorol. Soc.* 84 (2003) 767–776.
- [26] V. Cooray, M. Fernando, V. Scuka, T. Sorensen, A. Pedersen, The fine structure of positive return stroke radiation fields—a collaborative study between researchers from Sweden and Denmark, in: *Proceedings of the International Conference on Lightning Protection*, Birmingham, England, 1998.
- [27] D.M. Mach, W.D. Rust, Two-dimensional velocity, optical risetime, and peak current estimates for natural positive lightning return strokes, *J. Geophys. Res.* 98 (1993) 2635–2638.
- [28] V. Shostak, W. Janischewskij, A.M. Hussein, B. Kordi, Electromagnetic fields of lightning strikes to a tall tower: a model that accounts for upward-connecting discharges, in: *Proceedings of the 25th International Conference on Lightning Protection*, Rhodes, Greece, 2000, pp. 60–65.
- [29] V. Shostak, W. Janischewskij, A.M. Hussein, J.S. Chang, B. Kordi, Return stroke current modeling of lightning striking a tall tower accounting for reflections within the growing channel and for upward-connecting discharges, in: *Proceedings of the 11th International Conference on Atmospheric Electricity*, Alabama, 1999, pp. 123–126.
- [30] W. Janischewskij, V. Shostak, A.M. Hussein, Comparison of lightning electromagnetic field characteristics of first and subsequent return strokes to a tall tower: 1. Magnetic field, in: *Proceedings of the 24th International Conference on Lightning Protection*, Birmingham, UK, 1998, pp. 245–251.

- [31] F. Rachidi, C.A. Nucci, On the Master, Uman, Lin, Standler and the modified transmission line lightning return stroke models, *J. Geophys. Res.* 95 (1990) 20389–20394.
- [32] V. Cooray, The modelling of positive return strokes in lightning flashes, *J. Atmos. Solar-Terrestrial Phys.* 62 (2000) 169–187.
- [33] V. Cooray, S. Lundquist, On the characteristics of some radiation fields from lightning and their possible origin in positive ground flashes, *J. Geophys. Res.* 87 (1982) 11203–11214.
- [34] V. Mazur, L.H. Ruhnke, Evaluation of the lightning protection system of the WSR-88D radar sites, Technical Report, National Severe Storms Laboratory, Norman, 2001.
- [35] V.A. Rakov, M.A. Uman, *Lightning: Physics and Effects*, Cambridge University Press, Cambridge, 2003, p. 687.